Nanostructures

DOI: 10.1002/ange.200503762

Sonochemical Formation of Single-Crystalline Gold Nanobelts**

Jianling Zhang, Jimin Du, Buxing Han, Zhimin Liu, Tao Jiang, and Zhaofu Zhang*

In recent years, metal nanostructures with specific size and morphology have been the focus of intensive research owing to their potential applications in the fabrication of electronic, optical, optoelectronic, and magnetic devices. The intrinsic properties of a metal nanostructure can be tuned by controlling its size, shape, and crystallinity.[1] One-dimensional (1D) nanostructures such as nanowires, nanotubes, and nanobelts (or nanoribbons) have attracted much attention on account of their numerous potential applications in science and engineering.[2] In particular, the planar nanostructures of nanobelts have been intensively studied because the nanobelts may represent a good system for examining dimensionally confined transport phenomena.[3] However, there are very few reports on the synthesis of metal nanobelts (or nanoribbons), although many processes have been successfully applied to the synthesis of oxide,[4] sulfide,[5] and carbon[6] nanobelts. Xia et al. reported the synthesis of silver nanobelts by heating an aqueous dispersion of spherical colloids of silver with a diameter of 3.5 nm under reflux.[7] Qian and coworkers prepared ultrathin nickel[8] and tellurium nanobelts[9] by a hydrothermal method.

Ultrasound has become an important tool for the synthesis of metal nanoparticles in recent years.[10] It is well known that ultrasonic irradiation of liquids has a variety of physical and chemical effects derived from acoustic cavitation, and can provide a unique method for driving chemical reactions under extreme conditions.[11] The sonochemical method is advantageous as it is nonhazardous, rapid in reaction rate, and produces very small metal particles. Unfortunately, metal nanoparticles prepared by sonochemical reduction generally have multiple shapes and wide size distributions. To solve these problems, surfactants and coexisting alcohols are usually used in the sonochemical process to control the particle shape and size.[12]

More recently, with the advent of green chemistry, the biosynthesis of nanostructures has attracted much interest in materials science because of the minimized adverse environmental effects.[13] The biomaterial templating technique has been demonstrated to be an efficient method for directing the synthesis and manufacture/assembly of artificial nanostructures of crystalline inorganic materials under environmentally benign conditions.[14] Many biomaterials, such as DNA, viruses, and sugars, have been used as biological templates to grow nanostructures of noble metals,[15] oxides,[16] sulfides,[17] and metal alloys.[18]

It is interesting to fabricate various gold nanostructures, which may find practical applications in nanodevices, and the syntheses of nanorods,[19] nanowires,[20] nanorings,[21] nanocubes,[22] and nanoplates[23] have been reported. Herein, we report a method for synthesizing single-crystalline gold nanobelts through the combination of ultrasound irradiation and a biological directing agent. In this route, an aqueous solution of $HAuCl_4$ containing α-D-glucose was ultrasonically irradiated to produce gold nanobelts. This method has some clear advantages: it is green, simple, rapid, and can be performed under ambient conditions.

The major reactions that occur in the sonolysis of an aqueous solution containing $HAuCl_4$ and α-D-glucose can be summarized by the following steps [Eq. (1)–(4)]:[24]

$$H_2O \rightarrow H^{\cdot} + {}^{\cdot}OH \quad (1)$$

$$\text{sugar} \rightarrow \text{pyrolysis radicals} \quad (2)$$

$$Au^{III} + \text{reducing radicals} \rightarrow Au^0 \quad (3)$$

$$n\,Au^0 \rightarrow Au_n \quad (4)$$

The two reducing radicals, generated from the reaction of α-D-glucose with primary radicals such as the hydroxyl radical and the hydrogen radical originating from water molecules [Eq. (1)], and from the direct decomposition of glucose at the interfacial region between the collapsing cavities and the bulk water [Eq. (2)], are effective for the reduction of $AuCl_4^-$ [Eq. (3)] followed by particle growth [Eq. (4)].

Figure 1a and b show representative scanning electron microscopy (SEM) images of the as-synthesized gold prod-

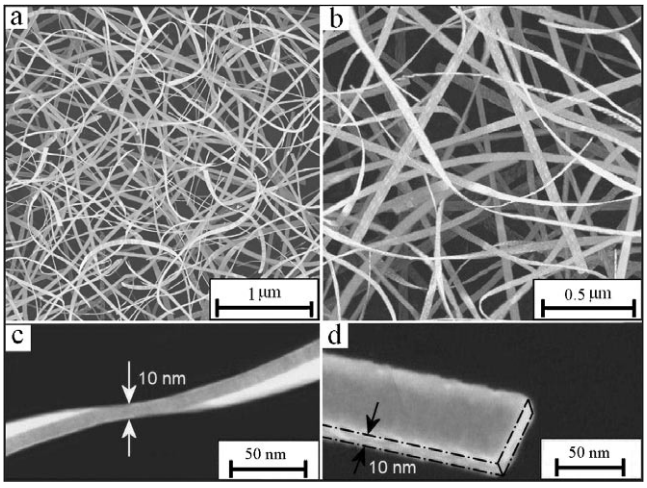

Figure 1. a,b) SEM images and c,d) high-magnification SEM images of as-synthesized gold nanobelts; $[HAuCl_4] = 50\ mg\,mL^{-1}$, [α-D-glucose] = 0.2 M, ultrasound time = 1 h.

[*] Dr. J. Zhang, J. Du, Prof. B. Han, Dr. Z. Liu, Dr. T. Jiang, Dr. Z. Zhang
Center for Molecular Sciences, Institute of Chemistry
Chinese Academy of Sciences
Beijing 100080 (P.R. China)
Fax: (+86) 106-255-9373
E-mail: Hanbx@iccas.ac.cn

[**] This work was supported by the National Natural Science Foundation of China (20403021).

Supporting information for this article is available on the WWW under http://www.angewandte.org or from the author.

ucts. The initial concentrations of $HAuCl_4$ and α-D-glucose were 50 mg mL^{-1} and 0.2 M, respectively, and the ultrasound irradiation time was 1 h. The geometrical configuration of the nanobelts is clearly displayed in the SEM images. The gold nanobelts typically have a width of 30–50 nm and a length of several micrometers. They are highly flexible and can bend > 90° without breaking. To further analyze the characteristics of the nanobelts, high-magnification SEM images are given in Figure 1c and d. Typical nanobelts have smooth side edges and an even thickness of approximately 10 nm. Figure 1d shows the tip surface of a typical nanobelt, in which a rectangular-shaped cross section is observed, similar to those of semiconducting oxide nanobelts.[4f]

The detailed microstructure of the gold nanobelts was further characterized by transmission electron microscopy (TEM; see Figure 2a). The TEM images also reveal that the

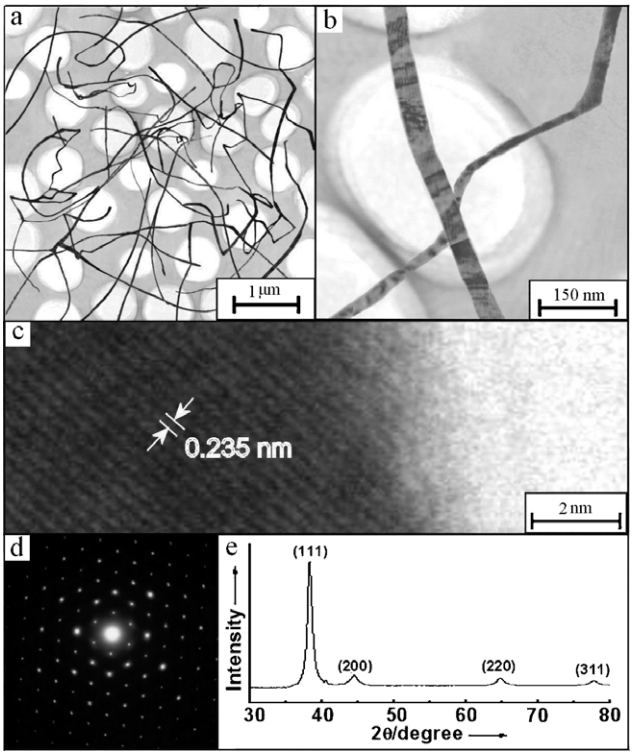

Figure 2. TEM images with a) lower and b) higher magnification, c) HRTEM image, d) SAED pattern, and e) XRD pattern of gold nanobelts; [$HAuCl_4$] = 50 mg mL^{-1}, [α-D-glucose] = 0.2 M, ultrasound time = 1 h.

width of the gold products is in the range 30–50 nm and that the length can reach several micrometers. The characteristic variation in lateral dimension associated with a belt is clearly observed from the bending in the middle of a 1D nanostructure (see Figure 2b). A high-resolution TEM (HRTEM) image of typical nanobelts is shown in Figure 2c, which was obtained with the incident electron beam perpendicular to the wide surface of the nanobelt. The measured interplanar spacing for all the lattice fringes is 0.235 nm, which corresponds to the (111) lattice plane of face-centered-cubic (fcc) gold. Figure 2d presents the selected-area electron diffraction (SAED) pattern of the gold nanobelts, which was obtained by focusing the electron beam on a nanobelt lying flat on the TEM grid. A diffraction pattern with hexagonal symmetry is generated, which demonstrates that the gold nanobelt is a single crystal with preferential growth along the Au[111] direction.[23a,25] The SAED patterns are essentially identical over the entire belt, thus revealing the single-crystalline and structurally uniform nature of the nanobelts. X-ray diffraction (XRD) gives further support to the phase structure of the gold nanobelts. The four diffraction peaks shown in Figure 2e correspond to the (111), (200), (220), and (311) diffraction peaks of metallic gold, which indicates that the products are composed of pure crystalline gold. The gold nanobelts were additionally characterized by energy-dispersive X-ray spectroscopy (EDS) and X-ray photoelectron spectroscopy (XPS), which confirmed that the nanobelts are pure gold (see Supporting Information).

To investigate the details of the sonochemical formation of gold nanobelts, we studied the different stages in the growth of gold by changing the reaction time (see Figure 3).

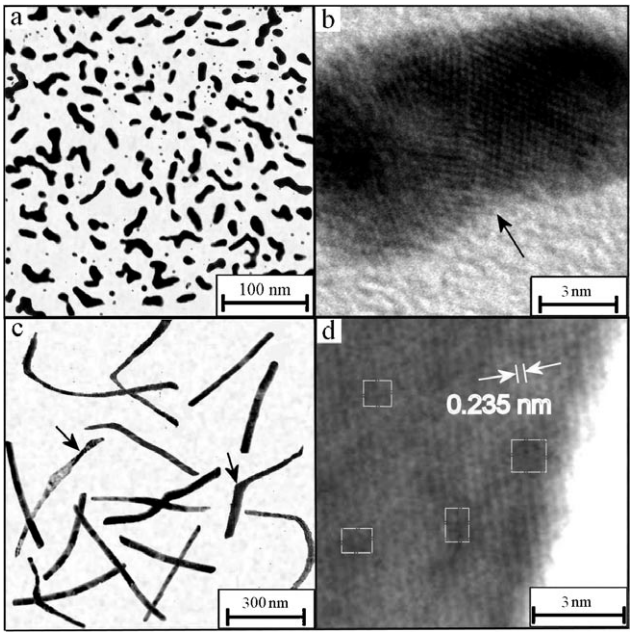

Figure 3. TEM images of gold after ultrasound irradiation for a) 10 and c) 30 min, and the corresponding HRTEM images (b,d); [$HAuCl_4$] = 50 mg mL^{-1}, [α-D-glucose] = 0.2 M. The arrow in (b) marks the junction of two neighboring gold particles; the arrows in (c) reveal characteristic variations in lateral dimensions associated with a beltlike shape; the rectangles in (d) show structures that are not fully crystallized.

When the irradiation time was as short as 10 min, directional aggregates of gold were formed (8 nm average width; Figure 3a). The HRTEM image of the same sample (Figure 3b) shows that two neighboring gold particles are fused at their junction and exhibit a polycrystalline structure. When the ultrasound time was prolonged to 30 min, short 1D nanostructures of gold with an average width and length of 20 nm and 0.5 μm, respectively, were obtained. The beltlike shape is clearly observed from the curving and bending in the

middle of these short 1D nanostructures (marked with arrows in Figure 3c). Figure 3d is the corresponding HRTEM image. By comparison with Figure 2c, it is noted that the structure of these short nanobelts is the same as that of the nanobelts obtained after ultrasound irradiation for 1 h. However, these short nanobelts are not fully crystallized and are somewhat disordered (see rectangles marked in Figure 3d). The longer ultrasound irradiation time gives rise to high-quality single-crystalline nanobelts (see Figure 2). It can therefore be concluded that the nanobelts grow from the merged particles. We reasonably speculate that the nanobelt formation process has following steps: 1) gold nuclei are formed and grow into nanoparticles; 2) the gold nanoparticles are directionally aggregated, melted, and then bound to each other (actually a recrystallization process); and 3) growth along the Au[111] direction and further crystallization result in the single-crystalline nanobelt structure. Note that some spherical particles with smaller sizes (2–3 nm) were observed in the early stage of the reaction (10 min, see Figure 3a). We suggest that the anisotropic growth of gold nanobelts follows the Ostwald ripening process at the expense of the small gold nanoparticles.[1a,26]

The above formation process of the gold nanobelts is similar to that of single-crystalline selenium nanowires prepared by the sonication method.[27] As for the reason for the formation of nanobelts, we believe that α-D-glucose can selectively adsorb onto the crystallographic planes of gold,[28] thus serving as a directing agent and kinetically controlling the anisotropic growth of gold. To understand the function of α-D-glucose, we conducted a contrast experiment with β-cyclodextrin, which is a cyclic oligomer containing seven α-D-glucose units. The other conditions were the same as those for preparing the gold nanobelts with α-D-glucose. The results showed that only spherical particles with a diameter of approximately 30 nm were obtained in the presence of β-cyclodextrin (see Supporting Information). This finding indicates that α-D-glucose plays a key role in the formation of gold nanobelts. We also found that the formation of gold nanobelts depends on the concentration of α-D-glucose. When its concentration was as low as 0.05 M, only gold particles with a size of approximately 40 nm were obtained (see Supporting Information). The reason may be that the capping effect of the glucose in the dilute solution is not sufficient for the effective coverage or passivation of gold facets, thus resulting in the formation of nanoparticles instead of nanobelts. In addition, cavitations and shock waves created by ultrasound irradiation can not only accelerate solid particles to high velocities and drive them together to induce effective melting at the point of interparticle collision,[27,29] but may also enhance the entanglement and rearrangement of the α-D-glucose molecules on gold crystals. All these effects induced by ultrasound may partly contribute to the final formation of single-crystalline gold nanobelts.

Gold nanomaterials show unique optical properties as a result of surface plasmon resonance. It is well known that spherical gold nanoparticles exhibit a single absorption band at 520 nm, whereas anisotropic gold particles show two surface plasmon resonance absorption peaks that are characteristic of the short (transverse band) and long (longitudinal band) axes of these systems.[30] Spectrum a in Figure 4 shows the UV/Vis absorption spectrum of gold nanobelts suspended in water. One peak corresponding to the short axes of the nanobelts appears at about 544 nm; the other peak increases into the IR region with no indication of leveling off, as also observed for gold nanowires,[31] and can be attributed to the long aspect ratio of the gold nanobelts. For gold particles with a diameter of approximately 30 nm synthesized in the presence of β-cyclodextrin, the characteristic surface plasmon band is observed at $\lambda_{max} = 530$ nm (spectrum b in Figure 4). Thus, the appearance of the absorption band actually mirrors the appearance of the different nanostructures of gold.

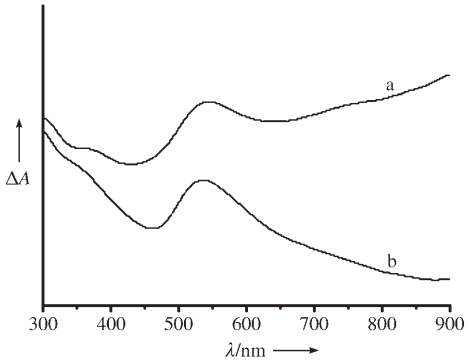

Figure 4. UV/Vis spectra of a) gold nanobelts and b) gold nanospheres synthesized in the presence of α-D-glucose (a) and β-cyclodextrin (b), respectively; $[HAuCl_4] = 50\ mg\,mL^{-1}$, [α-D-glucose] = 0.2 M, [β-cyclodextrin] = 0.2 M, ultrasound time = 1 h.

In conclusion, we have successfully synthesized single-crystalline gold nanobelts by a sonochemical route in the presence of α-D-glucose. This method is simple, convenient, economical, and environmentally benign, and can be performed under ambient conditions. The gold nanobelts have potential for incorporation into functional electronic, optoelectronic, or sensing devices, which could lead to extreme miniaturization and enhanced performance. In addition, such gold nanobelts can be used as building blocks to form a variety of functional nanostructures with special physical and chemical properties. This method may be applied to the synthesis of other nanosized metal materials.

Experimental Section

$HAuCl_4 \cdot 4H_2O$, α-D-glucose, and β-cyclodextrin were provided by the Beijing Analytical Instrument Factory. Deionized water was used. In a typical experiment, an aqueous solution of $HAuCl_4$ ($50\ mg\,mL^{-1}$) was placed in a sonication vessel, and then mixed with the desired amount of α-D-glucose (or β-cyclodextrin). The solution was exposed to high-intensity ultrasound irradiation (40 kHz, 100 W) for 10–60 min. The products were collected after deposition and aging, and then washed with deionized water.

The morphologies of the products were characterized by SEM (Hitachi-530) and TEM (Tecnai 20, Philips). The HRTEM images and SAED patterns were recorded on a JEOL JEM-2010 transmission electron microscope operating at 200 kV. XRD analysis of the samples was carried out by using an X-ray diffractometer (Model D/MAX2500, Rigaku) with $Cu_{K\alpha}$ radiation. X-ray photoelectron spectra

were collected by an ESCALab220i-XL spectrometer operating at 15 kV and 20 mA, at a pressure of 3×10^{-9} mbar with $Al_{K\alpha}$ as the exciting source ($h\nu = 1486.6$ eV). UV/Vis absorption spectra of gold particles suspended in water were collected by a TU-1201 Model spectrophotometer (Beijing General Instrument Company).

Received: October 24, 2005
Published online: January 3, 2006

Keywords: crystal growth · gold · nanostructures · ultrasound

[1] a) R. Jin, Y. Cao, C. A. Mirkin, K. L. Kelly, G. C. Schatz, J. G. Zheng, *Science* **2001**, *294*, 1901; b) M. A. El-Sayed, *Acc. Chem. Res.* **2001**, *34*, 257.
[2] a) Z. L. Wang, R. P. Gao, Z. W. Pan, Z. R. Dai, *Adv. Eng. Mater.* **2001**, *3*, 657; b) Y. Xia, P. Yang, Y. Sun, Y. Wu, B. Mayers, B. Gates, Y. Yin, F. Kim, H. Yan, *Adv. Mater.* **2003**, *15*, 353; c) Z. L. Wang, *Adv. Mater.* **2003**, *15*, 432; d) G. A. Baker, *Adv. Mater.* **2005**, *17*, 639.
[3] a) Z. W. Pan, Z. R. Dai, Z. L. Wang, *Science* **2001**, *291*, 1947; b) W. Shi, H. Peng, N. Wang, C. P. Li, L. Xu, C. S. Lee, R. Kalish, S.-T. Lee, *J. Am. Chem. Soc.* **2001**, *123*, 11095.
[4] a) X. Y. Kong, Y. Ding, R. Yang, Z. L. Wang, *Science* **2004**, *303*, 1348; b) X. G. Wen, S. H. Wang, Y. Ding, Z. L. Wang, S. H. Yang, *J. Phys. Chem. B* **2005**, *109*, 215; c) Z. L. Wang, *Annu. Rev. Phys. Chem.* **2004**, *55*, 159; d) J. Liu, Q. Li, T. Wang, D. Yu, Y. Li, *Angew. Chem.* **2004**, *116*, 5158; *Angew. Chem. Int. Ed.* **2004**, *43*, 5048; e) Z. R. Dai, Z. W. Pan, Z. L. Wang, *Adv. Funct. Mater.* **2003**, *13*, 9; f) B. C. Cheng, Y. H. Xiao, G. S. Wu, L. D. Zhang, *Adv. Funct. Mater.* **2004**, *14*, 913; g) X.-S. Fang, C.-H. Ye, L.-D. Zhang, T. Xie, *Adv. Mater.* **2005**, *17*, 1661; h) R. Ma, Y. Bando, L. Zhang, T. Sasaki, *Adv. Mater.* **2004**, *16*, 918.
[5] a) X. S. Fang, C. H. Ye, L. D. Zhang, Y. H. Wang, Y. C. Wu, *Adv. Funct. Mater.* **2005**, *15*, 63; b) C. Ma, D. Moore, J. Li, Z. L. Wang, *Adv. Mater.* **2003**, *15*, 228; c) W. Zhang, L. Xu, K. Tang, F. Li, Y. Qian, *Eur. J. Inorg. Chem.* **2005**, 653; d) W.-T. Yao, S.-H. Yu, L. Pan, J. Li, Q.-S. Wu, L. Zhang, J. Jiang, *Small* **2005**, *1*, 320.
[6] a) Z. Kang, E. Wang, B. Mao, Z. Su, L. Gao, S. Lian, L. Xu, *J. Am. Chem. Soc.* **2005**, *127*, 6534; b) J. Liu, M. Shao, Q. Tang, S. Zhang, Y. Qian, *J. Phys. Chem. B* **2003**, *107*, 6329.
[7] Y. Sun, B. Mayers, Y. Xia, *Nano Lett.* **2003**, *3*, 675.
[8] Z. Liu, S. Li, Y. Yang, S. Peng, Z. Hu, Y. Qian, *Adv. Mater.* **2003**, *15*, 1946.
[9] M. Mo, J. Zeng, X. Liu, W. Yu, S. Zhang, Y. Qian, *Adv. Mater.* **2002**, *14*, 1658.
[10] a) M. Ashokkumar, F. Grieser, *Rev. Chem. Eng.* **1999**, *15*, 41; b) S. Zhu, H. Zhou, M. Hibino, I. Honma, M. Ichihara, *Adv. Funct. Mater.* **2005**, *15*, 381; c) T. Gao, T. H. Wang, *Chem. Commun.* **2004**, 2558; d) T. Gao, T. H. Wang, *Chem. Mater.* **2005**, *17*, 887; e) H. S. Xia, Q. Wang, *Chem. Mater.* **2002**, *14*, 2158; f) A. Gedanken, X. Tang, Y. Wang, N. Perkas, Y. Koltypin, M. V. Landau, L. Vradman, M. Herskowitz, *Chem. Eur. J.* **2001**, *7*, 4546.
[11] K. S. Suslick, G. J. Price, *Annu. Rev. Mater. Sci.* **1999**, *29*, 295.
[12] a) K. Barbour, M. Ashokkumar, R. A. Caruso, F. Grieser, *J. Phys. Chem. B* **1999**, *103*, 9231; b) X.-F. Qiu, J.-J. Zhu, H.-Y. Chen, *J. Cryst. Growth* **2003**, *257*, 37; c) K. Okitsu, A. Yue, S. Tanabe, H. Matsumoto, Y. Yobiko, *Langmuir* **2001**, *17*, 7717.
[13] S. Mann, *Nature* **1993**, *365*, 499.
[14] a) J. Aizenberg, D. A. Muller, J. L. Grazul, D. R. Hamann, *Science* **2003**, *299*, 1205; b) C. B. Mao, D. J. Solis, B. D. Reiss, S. T. Kottmann, R. Y. Sweeney, A. Hayhurst, G. Georgiou, B. Iverson, A. M. Belcher, *Science* **2004**, *303*, 213; c) H. Liang, T. E. Angelini, P. V. Braun, G. C. L. Wong, *J. Am. Chem. Soc.* **2004**, *126*, 14157.
[15] a) J. L. Gardea-Torresdey, J. G. Parsons, E. Gomez, J. Peralta-Videa, H. E. Troiani, P. Santiago, M. Jose Yacaman, *Nano Lett.* **2002**, *2*, 397; b) P. Mukherjee, A. Ahmad, D. Mandal, S. Senapati, S. R. Sainkar, M. I. Khan, R. Parishcha, P. V. Ajaykumar, M. Alam, R. Kumar, M. Sastry, *Nano Lett.* **2001**, *1*, 515; c) Z. M. Qi, H. S. Zhou, N. Matsuda, I. Honma, K. Shimada, A. Takatsu, K. Kato, *J. Phys. Chem. B* **2004**, *108*, 7006; d) Y. Liu, K. B. Male, P. Bouvrette, J. H. T. Luong, *Chem. Mater.* **2003**, *15*, 4172.
[16] a) C. E. Fowler, W. Shenton, G. Stubbs, S. Mann, *Adv. Mater.* **2001**, *13*, 1266; b) W. Shenton, S. Mann, H. Cölfen, A. Bacher, M. Fischer, *Adv. Mater.* **2001**, *13*, 442; c) T. Douglas, V. T. Stark, *Inorg. Chem.* **2000**, *39*, 1828.
[17] a) C. T. Dameron, R. N. Reese, R. K. Mehra, A. R. Kortan, P. J. Carroll, M. L. Steigerwald, L. E. Brus, D. R. Winge, *Nature* **1989**, *338*, 596; b) M. Kowshik, W. Vogel, J. Urban, S. K. Kulkarni, K. M. Paknikar, *Adv. Mater.* **2002**, *14*, 815; c) K. K. W. Wong, S. Mann, *Adv. Mater.* **1996**, *8*, 928.
[18] B. D. Reiss, C. Mao, D. J. Solis, K. S. Ryan, T. Thomson, A. M. Belcher, *Nano Lett.* **2004**, *4*, 1127.
[19] a) F. Kim, J. H. Song, P. Yang, *J. Am. Chem. Soc.* **2002**, *124*, 14316; b) D. A. Zweifel, A. Wei, *Chem. Mater.* **2005**, *17*, 4256; c) J. Y. Chang, H. M. Wu, H. Chen, Y. C. Liang, W. H. Tan, *Chem. Commun.* **2005**, 1092; d) J. H. Song, F. Kim, D. Kim, P. D. Yang, *Chem. Eur. J.* **2005**, *11*, 910.
[20] a) E. Tosatti, S. Prestipino, *Science* **2000**, *289*, 561; b) T. Sainsbury, D. Fitzmaurice, *Chem. Mater.* **2004**, *16*, 2174; c) T. O. Hutchinson, Y. P. Liu, C. Kiely, C. J. Kiely, M. Brust, *Adv. Mater.* **2001**, *13*, 1800.
[21] a) Q. Sun, Q. Wang, P. Jena, R. Note, J. Z. Yu, Y. Kawazoe, *Phys. Rev. B* **2004**, *70*, 245411; b) Y. Sun, Y. Xia, *Adv. Mater.* **2003**, *15*, 695.
[22] a) Y. Sun, Y. Xia, *Science* **2002**, *298*, 2176; b) J. Chen, B. Wiley, Z.-Y. Li, D. Campbell, F. Saeki, H. Cang, L. Au, J. Lee, X. Li, Y. Xia, *Adv. Mater.* **2005**, *17*, 2255.
[23] a) X. Sun, S. Dong, E. Wang, *Angew. Chem.* **2004**, *116*, 6520; *Angew. Chem. Int. Ed.* **2004**, *43*, 6360; b) D. Brohm, S. Metzger, A. Bhargava, O. Müller, F. Lieb, H. Waldmann, *Angew. Chem.* **2002**, *114*, 203; *Angew. Chem. Int. Ed.* **2002**, *41*, 195.
[24] a) K. Okitsu, Y. Mizukoshi, H. Bandow, A. T. Yamamoto, Y. Nagata, Y. Maeda, *J. Phys. Chem. B* **1997**, *101*, 5470; b) Y. Mizukoshi, E. Takagi, H. Okuno, R. Oshima, Y. Maeda, Y. Nagata, *Ultrason. Sonochem.* **2001**, *8*, 1.
[25] Y. Zhou, C. Y. Wang, Y. R. Zhu, Z. Y. Chen, *Chem. Mater.* **1999**, *11*, 2310.
[26] a) A. R. Roosen, W. C. Carter, *Physica A* **1998**, *261*, 232; b) Y. Sun, Y. Yin, B. Mayers, T. Herricks, Y. Xia, *Chem. Mater.* **2002**, *14*, 4736.
[27] H. Zhang, D. Yang, Y. Ji, X. Ma, J. Xu, D. Que, *J. Phys. Chem. B* **2004**, *108*, 1179.
[28] a) R. Holze, M. Beltowska-Brzezinska, *Electrochim. Acta* **1985**, *30*, 937; b) P. S. Vukusic, G. W. Bradberry, J. R. Sambles, *Surf. Sci.* **1992**, *277*, L34; c) R. A. Caruso, M. Ashokkumar, F. Grieser, *Langmuir* **2002**, *18*, 7831.
[29] a) S. J. Doktycz, K. S. Suslick, *Science* **1990**, *247*, 1067; b) H. Wang, Y.-N. Lu, J.-J. Zhu, H.-Y. Chen, *Inorg. Chem.* **2003**, *42*, 6404.
[30] a) N. Malikova, I. Pastoriza-Santos, M. Schierhorn, N. A. Kotov, L. M. Liz-Marzán, *Langmuir* **2002**, *18*, 3694; b) T. K. Sau, C. J. Murphy, *Langmuir* **2004**, *20*, 6414; c) Z. Zhong, J. Luo, T. P. Ang, J. Highfield, J. Lin, A. Gedanken, *J. Phys. Chem. B* **2004**, *108*, 18119.
[31] a) C. D. Chen, Y. T. Yeh, C. R. C. Wang, *J. Phys. Chem. Solids* **2001**, *62*, 1587; b) S. S. Chang, C. W. Shih, C. D. Chen, W. C. Lai, C. R. C. Wang, *Langmuir* **1999**, *15*, 701; c) L. Pei, K. Mori, M. Adachi, *Langmuir* **2004**, *20*, 7837.

